Physica E 144 (2022) 115448

Contents lists available at ScienceDirect

Physica E: Low-dimensional Systems and Nanostructures

journal homepage: www.elsevier.com/locate/physe

Magnetic barrier and temperature effects on optical and dynamic properties of exciton-polaron in monolayers transition metal dichalcogenides

A.K. Teguimfouet [a], C. Kenfack-Sadem [b,c,*], A. Kenfack-Jiotsa [d], F.C. Fobasso Mbognou [b], M. El-Yadri [e,**], L.M. Pérez [f], D. Laroze [g], E. Feddi [e,h]

[a] Laboratoire de Mécanique, Matériaux et Structures, Département de Physique, Université de Yaoundé 1, BP 812, Yaoundé, Cameroon
[b] Laboratory of Condensed Matter-Electronics and Signal Processing (LAMACET), Department of Physics, University of Dschang, P.O.Box 67, Dschang, Cameroon
[c] International Chair in Mathematical Physics and Applications, University of Abomey-Calavi, Cotonou, Benin
[d] Département de Physique, Ecole Normale Supérieure, Université de Yaoundé 1, BP 42, Yaoundé, Cameroon
[e] Group of Optoelectronic of Semiconductors and Nanomaterials, ENSAM, Mohammed V University in Rabat, Morocco
[f] Departamento de Física, FACI, Universidad de Tarapacá, Casilla 7 D, Arica, Chile
[g] Instituto de Alta Investigación, CEDENNA, Universidad de Tarapacá, Casilla 7 D, Arica, Chile
[h] Institute of Applied Physics, Mohammed VI Polytechnic University, Lot 660, Hay Moulay Rachid Ben Guerir, 43150, Morocco

ARTICLE INFO

Keywords:
Exciton-polaron
TMDs
Magnetic barrier
Temperature

ABSTRACT

We theoretically investigate the properties of exciton-polaron moving through a magnetic barrier in monolayers (1Ls) transition metal dichalcogenides (TMDs): MoS_2, WS_2, $MoSe_2$, and WSe_2. We find that the exciton-polaron has the highest ground state energy in WS_2 and the lowest one in $MoSe_2$. It is seen that the magnetic barrier stabilizes the excitonic polaron system subjected to thermal perturbation. We demonstrate that the entropy of the system is very sensitive to the type of monolayers TMDs, the length scale of the barrier, the temperature. We observe that the higher the magnetic length, the greater the disorder in exciton-polaron system and the highest entropy is in $MoSe_2$. Also, the mobility and the lifetime of exciton-polaron decrease with the enhancement of the magnetic length. We observe the highest mobility and lifetime in WS_2. Moreover, We show that the optical absorption appears when the photon energy is more than twice phonon energy and the absorption coefficient is higher when the incident photon induces an in plane field. MoS_2 presents the highest amplitude of optical absorption.

1. Introduction

In both molecular lattices (agregats) and large molecules, excitons play important roles as transmitting of informations, carrying energy and activating some chemical reactions. More recently, excitons in monolayers (1Ls) transition metal dichalcogenides (TMDs) [1,2] have grown very rapidly due to the optical and electronic characteristics. These structures are considered as one of the most interesting 2D materials due to their large band of applications such as fabrication of electronic devices [3], spintronics and valleytronic [4], preparation of qubit [5]. Additionally, the magneto-optical mechanisms of 1Ls TMDs [6–8] have stimulated some new opportunities for applications where a comprehensive insight of the action of a magnetic field affecting the excitons is desired. Indeed, excitons in TMD's monolayers submitted to a magnetic field show interesting optical and electronic characteristics [9–11] due to the large binding energy of the excitons [12–14]. It has been shown that the external magnetic field applied to a 1L TMD provides an experimental understanding of the characteristics of excitons, such as their spatial extent [15,16].

Unfortunately, in practice, the exciton does not spread freely, but it is constantly interacting with the other degrees of freedom in the crystal lattice. At a finite temperature, a strong coupling appears with low internal vibrations so called as phonons or polaronic effects [17,18]. The main idea is to say that phonons cause random fluctuations of energy from each local state. Therefore, identifying the nature and properties of the exciton's motion appear to be a difficult task, crucial for

* Corresponding author. Laboratory of Condensed Matter-Electronics and Signal Processing (LAMACET), Department of Physics, University of Dschang, P.O.Box 67, Dschang, Cameroon.
** Corresponding author.
E-mail addresses: kevinsadem@yahoo.fr (C. Kenfack-Sadem), md.yadri@gmail.com (M. El-Yadri).

https://doi.org/10.1016/j.physe.2022.115448
Received 6 March 2022; Received in revised form 30 June 2022; Accepted 20 July 2022
Available online 27 August 2022

understanding its role in various transport processes.

The principle of exciton-polaron has been elaborated extensively by a number of authors who have demonstrated that the exciton behavior is modified according to the coupling with phonons [19–25]. In confined system, this interaction is more obvious and presents some interesting futures mainly in 2D materials. It has been thoroughly explored both theoretically and experimentally by several authors [26–30]. In low dimensional system, the interaction between electron-hole pair and phonon is recognized to change the real apparent mass of exciton and reduces its energy, leading to a shift of the energy difference. Confined particles are relevant in nanostructures applications [31–33], so, several potential models have been developed in order to describe and control the dynamics of quasiparticles. Several parameters as the width, the depth of Gaussian well and temperature turned out to be significant in the study of energy levels and lifetime of polaron [34]. In the latter, it is found that lifetime decays with temperature. Also, Li [35] revealed that one can adjust the polaron ground state lifetime by changing the temperature, the polaron radius, the pseudoharmonic potential and the external field. This is interesting for application in quantum computation.

Inspired by the invention of an exceptional optical and electronic system [36–38], the class of 2D monolayers TMDs has attracted the attention of the scientific community. The dynamics of excitons and carriers in monolayers TMDs were examined by absorption or reflectivity of the pump-probe experiences [39–43]. Owing to a high temporal resolution (∼100 fs), these experimental results have highlighted a complex dynamic generally described by multi-exponential decay times [44]. Wu et al. [45] examined the optical absorption of cross-layer excitons in TMD heterolayers, they showed a diversity of cross-layer excitons in the two directions of optical activity and energies occur at any given valley. It has been demonstrated that excitons between layers possess a long-lived and easily electro-tunable energy due to their spatially indirect character [46]. However, they continue to exhibit a fairly high electron-hole binding energy. Moreover, the large band gap confers to TMD materials the possibility of high charge carrier mobility and high absorption coefficient [47]. From the work of Li et al. [48], the optical absorption appears when the incident photon energy exceeds the energy of optical phonon. Also, Thilagam [49] studied the ground state energy and the mass change of exciton-polaron for some monolayers. It is shown that under impurity effect, the exciton is localized in a quantum well. In this nanostructure, the transport of excitons is mostly quasi-2D and the variation in the size of the exciton alters the impact of its interplay with phonons. Consequently, it is advisable to explore how the features of an exciton-polaron in TMDs subjected to magnetic barrier.

As mentioned by several authors, exciton-polarons are ideal candidates for transmitting information and carrying energy. This inspires us to derive the lifetime, mobility, Tsallis entropy and the optical absorption coefficient. These are important properties necessary to describe the behavior of exciton-polaron in TMDs in order to ameliorate and understand the transport properties. In this paper, we determine theoretically the above properties of exciton-polaron in various monolayer TMD materials under magnetic field characterized by a magnetic length scale. The paper is organized as follows: in Sec. 2, we present the theory in which we describe the model of exciton-polaron system and derive the analytical expressions while in Sec. 3, we present our main results on energy, lifetime, mobility, entropy and optical absorption coefficient for the common 1Ls TMDs ($MoSe_2$, WSe_2, WS_2, MoS_2). Finally, in Sec. 4, we provide the conclusion.

2. Theoretical model

2.1. Hamiltonian of the system

Let us consider the motion of an exciton through a panel depicting a 1L TMD which interacts with longitudinal optical (LO)-phonons in presence of a magnetic strength. The total Hamiltonian of the system can be written as:

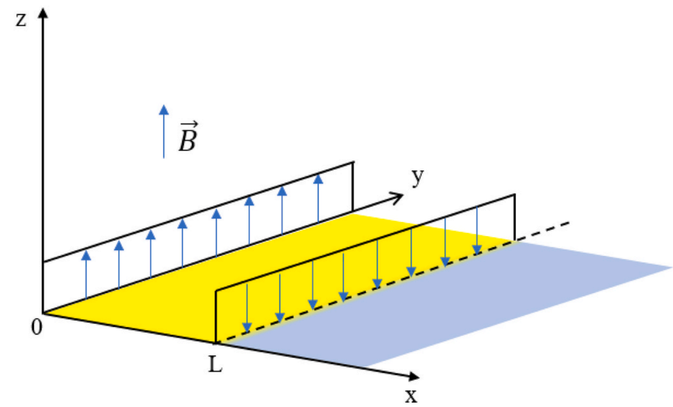

Fig. 1. Magnetic barrier using two long narrow magnetic stripes perpendicular to the monolayer TMD.

$$\widehat{H} = \widehat{H}_{ex}^{2D} + \widehat{H}_{ph} + \widehat{H}_{ex-ph}^{2D} \tag{1}$$

where $\widehat{H}_{ex}^{2D}$ is the Hamiltonian of electron and hole [50,51] taken here as:

$$\widehat{H}_{ex}^{2D} = \frac{1}{2m_e^*}\left(\vec{P}_e + e\vec{A}_e\right)^2 + \frac{1}{2m_h^*}\left(\vec{P}_h - e\vec{A}_h\right)^2 - \frac{e^2}{\varepsilon\left|\vec{\rho}_e - \vec{\rho}_h\right|} \tag{2}$$

where $\vec{P}_e$ ($\vec{P}_h$) is respectively the momentum vector of electron (hole) while $\vec{\rho}_e$ ($\vec{\rho}_h$) represents the electron (hole) position-vector in the xy-plane. m_e^* (m_h^*) is the effective mass of electron (hole). The last term of Eq. (2) is the coulomb interaction between electron and hole in the monolayer TMD. The magnetic barrier [52] is characterized by the field $\vec{B} = (0, 0, B_z)$ with $B_z(x) = B_0\, l_B[\delta(x) - \delta(x - L)]$. L is the barrier width taken at 150 nm, l_B indicates a length measure based on a standard magnetic flux field given by $B_0 = \hbar/(el_B^2)$.

From the definition of the Dirac delta function, this magnetic field can also take the form:

$$B_z = \begin{cases} B_0\, l_B\, ;\ if\ x = 0 \\ -B_0\, l_B\, ;\ if\ x = L \\ 0\, ;\ otherwise \end{cases} \tag{3}$$

Such barrier can be constructed as shows Ghosh et al. [53] and Fig. 1 illustrates the present case. Here, two long narrow magnetic stripes are placed perpendicular to the TMD layer respectively at $x = 0$ (with $B_0\, l_B$) and $x = L$ (with $-B_0\, l_B$). It is convenient to use the relation $\vec{B} = rot\vec{A}$ to obtain the vector potential of the magnetic barrier as $\vec{A} = (0, A_y, 0)$:

$$A_y(x) = B_0\, l_B\, [\Theta(x) - \Theta(x - L)] = \begin{cases} A\, ; & 0 < x < L \\ 0\, ; & otherwise \end{cases} \tag{4}$$

where $A = \hbar/(el_B)$ and Θ is the Heaviside function.

The phonon energy operator appear as:

$$\widehat{H}_{ph} = \sum_q \hbar\omega\, b_q^+ b_q \tag{5}$$

with b_q^+ and b_q denote the creation and annihilation operators of phonon, q the phonon wave vector with component $q_{//}$ in the xy-plane.

The last term of Eq. (1) stands for the Hamiltonian of exciton-phonon interaction given by Ref. [49]:

$$\widehat{H}_{ex-ph}^{2D} = \sum_{K,q_{//}} \Xi^{op}\left(q_{//}\right) C_{K+q_{//}}^+ C_K \left(b_{q_{//}} + b_{-q_{//}}^+\right) \tag{6}$$

where $C_K^+(C_K)$ denotes the creation (annihilation) operator of an exciton and K is the two-dimensional exciton wave vector. The exciton-optical phonon coupling function is taken as:

$$\Xi^{op}\left(q_{//}\right) = \left(D_c^{op} - D_v^{op}\right)\sqrt{\frac{\hbar q_{//}}{2\eta u S_{2D}}} \tag{7}$$

where S_{2D} represents the area of the layer plane, η denotes the area mass density and u is the sound velocity of the mode. D_c^{op} and D_v^{op} are respectively the deformation potential constant for electron-LO phonon coupling at some critical points (K, K') inside conduction band and the corresponding expression for hole in the valence band. These critical points are used to better estimate the polaronic effect on excitons.

Eq. (2) can be rewritten as:

$$\widehat{H}_{ex}^{2D} = \frac{\left(P_{e,x}^2 + P_{e,y}^2\right)}{2m_e^*} + \frac{\left(P_{h,x}^2 + P_{h,y}^2\right)}{2m_h^*} + \frac{e^2A^2}{2\mu^*} - \frac{e^2}{\varepsilon\left|\vec{\rho}_e - \vec{\rho}_h\right|} \tag{8}$$

μ^* is the effective exciton reduced mass given by:

$$\frac{1}{\mu^*} = \frac{1}{m_e^*} + \frac{1}{m_h^*} \tag{9}$$

Using the center of mass ($\vec{R} = \frac{m_e^*}{M^*}\vec{\rho}_e + \frac{m_h^*}{M^*}\vec{\rho}_h$) and the relative coordinate ($\vec{\rho} = \vec{\rho}_e - \vec{\rho}_h$),Eq. (8) becomes:

$$H_{ex}^{2D} = \frac{-\hbar^2}{2M^*}\nabla_R^2 - \left(\frac{\hbar^2}{2\mu^*}\nabla_\rho^2 + \frac{e^2}{\varepsilon\rho} - \frac{e^2A^2}{2\mu^*}\right) = H_R - H_{\rho,A} \tag{10}$$

$M^* = m_e^* + m_h^*$ represents the effective mass of an exciton. Let us check the 2D energy so that:

$$\widehat{H}_{ex}^{2D} = \sum_K \lambda C_K^+ C_K \tag{11}$$

This leads to the Schrodinger equation:

$$H_{ex}^{2D}\,\Psi_{ex} = \lambda\,\Psi_{ex} \tag{12}$$

The exciton wave function is considered as [51,54]:

$$\Psi_{ex} = \varphi(R)\,\varphi_{1s}(\rho) = \exp\left(i\vec{K}^*.\vec{R}\right)\sqrt{\frac{2}{\pi}}\,\frac{1}{a}\exp\left(-\frac{\rho}{a}\right) \tag{13}$$

with $\vec{K}^* = \vec{K} - \frac{e}{\hbar}\vec{A}$ and a the exciton Bohr radius.

For the center of mass, we have:

$$\frac{-\hbar^2}{2M^*}\nabla_R^2\,\varphi(R) = E(K, l_B)\,\varphi(R) \tag{14}$$

Thus

$$E(K, l_B) \approx E_g + \frac{\hbar^2}{2M^*}\left(K^2 + \frac{1}{l_B^2}\right) \tag{15}$$

E_g stands for the gap energy in the MX_2 monolayer.

Also, for the relative coordinate, we have:

$$-\langle\varphi_{1s}|H_{\rho,A}|\varphi_{1s}\rangle = -E_b + \frac{\hbar^2}{2\mu^* l_B^2} = E_b(l_B) \tag{16}$$

Here, E_b comes from the general formula $E_b = \frac{R_y}{(n-0.5)^2}$, $n = 1$ being the principal quantum number and R_y the Rydberg's constant. Then according to Eqs. (15) and (16), one gets:

$$\lambda = E(K, l_B) + E_b(l_B) \tag{17}$$

We obtain the expression of the exciton eigen energy as:

$$\lambda(K, \xi) = E_g + \frac{\hbar^2K^2}{2M^*} - E_b + \xi^2 \tag{18}$$

where ξ is the magnetic parameter given by:

$$\xi = \frac{\hbar}{l_B}\left(\frac{1}{2M^*} + \frac{1}{2\mu^*}\right)^{1/2} \tag{19}$$

It is seen that the magnetic barrier contributes on kinetic and binding energies respectively.

We use the following unitary transformation [49] to diagonalize the Hamiltonian of the system:

$$U_{ex} = \exp(iS) \tag{20}$$

with

$$S = \sum_{K,q_{//}} C_{K+q_{//}}^+ C_K\left[f_{ex}^*\left(K, q_{//}\right)b_{-q_{//}}^+ + f_{ex}\left(K, q_{//}\right)b_{q_{//}}\right] \tag{21}$$

U_{ex} is called the displaced-oscillator which is related to the phonon operators via Eq. (20). This transformation enables us to consider the dressed electron states due to the phonon field. It generates coherent states from the phonon vacuum. The variational functions f_{ex} and f_{ex}^* provide the phonon distribution function induced by the electron dynamics are determined as:

$$f_{ex}^*\left(K, q_{//}\right) = \frac{\Xi^{op}\left(q_{//}\right)}{\lambda\left(K + q_{//}, \xi\right) - \lambda(K, \xi) + \hbar\omega}\ and\ f_{ex}\left(K, q_{//}\right) = \frac{\Xi^{op}\left(q_{//}\right)}{\lambda\left(K + q_{//}, \xi\right) - \lambda(K, \xi) - \hbar\omega} \tag{22}$$

Theses functions shift the position of the vibrational modes quantifying the strength of the coupling between electron and lattice displacement.

According to Eq. (20), the transformed Hamiltonian gives:

$$\widehat{H}^T = U_{ex}^{-1}\widehat{H}U_{ex} \approx \widehat{H}_{ex}^{2D} + \widehat{H}_{ph} + \widehat{H}_{ex-ph}^{T2D} \tag{23}$$

where

$$\widehat{H}_{ex-ph}^{T2D} = \sum_{K,K',q_{//}}\left|\Xi^{op}\left(q_{//}\right)\right|^2\left[\frac{1}{\lambda\left(K + q_{//}, \xi\right) - \lambda(K, \xi) + \hbar\omega} - \frac{1}{\lambda\left(K + q_{//}, \xi\right) - \lambda(K, \xi) - \hbar\omega}\right]C_{K+q_{//}}^+ C_K C_{K'+q_{//}}^+ C_{K'} \tag{24}$$

We can now use the approximate diagonalized form of the Hamiltonian given by Eq. (23) to easily obtain the properties of the system like energy, mobility, entropy, optical absorption. Let us proceed by the calculation of entropy.

2.2. Tsallis entropy

In this section, we will evaluate the Tsallis entropy which depends of a degree (j) [55–58] as:

$$S_j = \frac{1 - \sum_{i=1}^{j} P_i^j}{j-1} \tag{25}$$

The probabilities are P_1 for ground state and P_2 for the first excited state given by:

$$P_1 = \frac{\left[1-\beta(1-j)E^0_{ex-pol}\right]^{\frac{1}{1-j}}}{Z_j} \ and\ P_2 = \frac{\left[1-\beta(1-j)E^1_{ex-pol}\right]^{\frac{1}{1-j}}}{Z_j} \tag{26}$$

and the partition function is defined as:

$$Z_j = \left[1-\beta(1-j)E^0_{ex-pol}\right]^{\frac{1}{1-j}} + \left[1-\beta(1-j)E^1_{ex-pol}\right]^{\frac{1}{1-j}} \tag{27}$$

the parameter j is a real number and represents the entropy degree and β is the inverse of temperature. E^0_{ex-pol} and E^1_{ex-pol} are respectively the fundamental state and the first excited level energies of the excitonic polaron. For the ground state, we have:

$$\frac{\hbar}{\tau} = \frac{M\left(D_c^{op}-D_v^{op}\right)^2}{4\pi\eta u} \int_0^{2\pi} \frac{d\theta}{\sqrt{\hbar^2K^2\cos^2\theta + 2M\hbar\omega}} \int_0^{\infty} dq_{//}\, \overline{n}\, q_{//}^2 \left[\delta\left(q_{//}-q_1\right) + \delta\left(q_{//}-q_2\right)\right] \tag{38}$$

$$E^0_{ex-pol} = \langle \Psi_0 | \widehat{H}^T | \Psi_0 \rangle \tag{28}$$

with the ground state wave function

$$|\Psi_0\rangle = C_K^+|0\rangle_k|0\rangle_{ph} \tag{29}$$

$|0\rangle_k$ and $|0\rangle_{ph}$ represent respectively the exciton's and phonon's vacuum state vectors. The state energies are obtained after straightforward calculations made in Eq. (23).

$$E^0_{ex-pol} = E_g + \left(\frac{\hbar^2K^2}{2M}\right)(1-\widetilde{G}_{ex2}) - E_b - G_{ex1} + \xi^2 \tag{30}$$

where

$$G_{ex1} = \frac{\pi\sqrt{\hbar\omega}\left(D_c^{op}-D_v^{op}\right)^2}{\sqrt{2}\,\hbar^2\eta u}\left(m_e^*+m_h^*\right)^{3/2} \ and\ \widetilde{G}_{ex2} = \frac{3\pi\left(D_c^{op}-D_v^{op}\right)^2}{4\sqrt{2}\,\hbar^2\eta u}\frac{\left(m_e^*+m_h^*\right)^{3/2}}{\sqrt{\hbar\omega}} \tag{31}$$

Using $|\Psi_1\rangle = C_K^+|1\rangle_k|0\rangle_{ph}$, the first excited state energy is obtain as:

$$E^1_{ex-pol} = 4E_g + 4\left(\frac{\hbar^2K^2}{2M}\right)(1-2\widetilde{G}_{ex2}) - 4E_b - 8G_{ex1} + 4\xi^2 \tag{32}$$

Inserting Eqs. (30) and (32) in Eq. (23), we obtain the entropy of the system.

2.3. Lifetime and mobility of the excitonic polaron

The form of energies obtained allows to investigate the lifetime of exciton-polaron in TMDs under magnetic field. To calculate this property, the following expression [59] is used:

$$\frac{\hbar}{\tau} = 2\pi\sum_q \left|\langle n_{q'}, K | H^{2D}_{ex-ph} | K, n_q\rangle\right|^2 \delta\left[\lambda_K - \lambda_{K+q} + \hbar\omega\right] \tag{33}$$

where

$$n_{q'} = n_q - 1 \tag{34}$$

For the ground state, we have:

$$\frac{\hbar}{\tau} = 2\pi\sum_q \left|\langle n_q - 1\, |\langle 0| C_K\, H^{2D}_{ex-ph}\, C_K^+\, |0\rangle | n_q\rangle\right|^2 \delta\left[\lambda_K - \lambda_{K+q} + \hbar\omega\right] \tag{35}$$

After averaging, Eq. (33) gives:

$$\frac{\hbar}{\tau} = 2\pi\sum_{q_{//}} \overline{n}\left(\Xi^{op}{}_{(q_{//})}\right)^2 \delta\left[\frac{\hbar^2}{2M}\left(q_{//}^2 + 2K.\,q_{//} - \frac{2M\hbar\omega}{\hbar^2}\right)\right] \tag{36}$$

According to Eq. (7) and converting the summation into integration, we obtain:

$$\frac{\hbar}{\tau} = \frac{M}{2\hbar\pi\eta u}\left(D_c^{op}-D_v^{op}\right)^2 \int_0^{2\pi} d\theta \int_0^{\infty} dq_{//}\, \overline{n}\, q_{//}^2\, \delta\left[q_{//}^2 + 2Kq_{//}\cos\theta - \frac{2M\hbar\omega}{\hbar^2}\right] \tag{37}$$

The Dirac function is transformed by using $\delta[g(q)] = \sum_i \frac{\delta(q-q_i)}{|g'(q_i)|}$ with q_i the roofs of g.

One gets:

where

$$q_1 = -k\cos\theta + \frac{1}{\hbar}\sqrt{\hbar^2K^2\cos^2\theta + 2M\hbar\omega} \ and\ q_2 = -k\cos\theta - \frac{1}{\hbar}\sqrt{\hbar^2K^2\cos^2\theta + 2M\hbar\omega} \tag{39}$$

The mean number of phonons in the ground state is taken from the quantum statistics as:

$$\overline{n} = \left[\exp\left(\beta E^0_{ex-pol}\right) - 1\right]^{-1} \tag{40}$$

The integration over $q_{//}$ gives:

$$\frac{\hbar}{\tau} = \frac{M\left(D_c^{op}-D_v^{op}\right)^2}{4\pi\eta u}\overline{n}\int_0^{2\pi}\frac{d\theta}{\sqrt{\hbar^2K^2\cos^2\theta + 2M\hbar\omega}}\left(q_1^2+q_2^2\right) \tag{41}$$

Thus, the expression of exciton-polaron lifetime is:

$$\frac{1}{\tau} = \frac{M\left(D_c^{op}-D_v^{op}\right)^2}{\hbar^3\pi\eta\, u}\overline{n}\int_0^{2\pi} d\theta\frac{\left(\hbar^2K^2\cos^2\theta + M\hbar\omega\right)}{\sqrt{\hbar^2K^2\cos^2\theta + 2M\hbar\omega}} \tag{42}$$

The mobility can be related to the mean number of phonons as [60]:

$$\mu \approx \frac{1}{\overline{n}} = \left[\exp\left(\beta E^0_{ex-pol}\right) - 1\right] \tag{43}$$

From here we observe that the lifetime and the mobility depend on the magnetic barrier and the TMD's characteristics. Thus, these properties can be affected by those parameters.

2.4. Optical absorption coefficient

When the exciton-polaron absorbs the light of frequency (Ω), the optical absorption coefficient $\Gamma(\hbar\Omega)$ is related to the probability $P(\hbar\Omega)$ of absorbing a photon in the ground state [61]:

Table 1
The performed physical parameters of 1L TMD materials used in calculation taken from Refs. [63,64]. $\hbar\omega$, D_c^{op}, D_v^{op}, E_b and E_g are given in unit of (eV); m_e and m_h are in unit of free electron mass.

Materials	m_e	m_h	$\hbar\omega$	D_c^{op}	D_v^{op}	E_b	E_g
$MoSe_2$	0.64	0.71	0.0365	5.2	4.9	0.174	1.56
WSe_2	0.39	0.51	0.0291	2.3	3.1	0.231	1.65
WS_2	0.31	0.42	0.0435	3.1	2.3	0.19	2.10
MoS_2	0.51	0.58	0.0443	5.8	4.6	0.313	1.87

$$\Gamma(\hbar\Omega)=\frac{\Omega}{cn\varepsilon_0\left(2E^2\right)}P(\hbar\Omega) \tag{44}$$

where ε_0 is the vacuum's permittivity, c is the light's velocity, n is the medium's refractive index and E represents the strength of the electric field vector of the incident photon. The transition probability is taken as [48]:

$$P(\hbar\Omega)=2\pi\sum_f\langle\Psi|\ V|\Psi_f\rangle\langle\Psi_f|\ V|\Psi\rangle\delta\left(E_0+\hbar\Omega-E_f\right)=2\mathrm{Re}\ R(\hbar\Omega) \tag{45}$$

Ψ (Ψ_f) is the ground state (possible final) wave function with energy E_0 (E_f) and $R(\hbar\Omega)$ is given by:

$$\mathrm{Re}\ R(\hbar\Omega)=\left(\frac{1}{\hbar\Omega}\right)^2\int_{-\infty}^{0}dt\ e^{-it(i\varepsilon+\hbar\Omega)}\langle\Psi|\ [H,V]_0[H,V]_t|\Psi\rangle \tag{46}$$

V is the time-dependent perturbation describes by the electric dipole interaction $V=eE.\,r$.

According to Eq. (8), the previous equation gives [62]:

$$\mathrm{Re}R(\hbar\Omega)=\left(\frac{e}{\hbar\Omega}\right)^2\int_{-\infty}^{0}dt\,e^{-it(i\varepsilon+\hbar\Omega)}\langle\Psi|E.\left\{\frac{p_e(0)}{m_e}+\frac{p_h(0)}{m_h}\right\}E.\left\{\frac{p_e(t)}{m_e}+\frac{p_h(t)}{m_h}\right\}|\Psi\rangle \tag{47}$$

Now, let us apply the unitary transformation:

$$\mathrm{Re}\ R(\hbar\Omega)=\left(\frac{e}{\hbar\Omega}\right)^2\int_{-\infty}^{0}dt\ e^{-it(i\varepsilon+\hbar\Omega)}\langle\Psi|E.\ U_{ex}^{-1}\left\{\frac{p_e(0)}{m_e}+\frac{p_h(0)}{m_h}\right\}U_{ex}\ E.\ U_{ex}^{-1}\left\{\frac{p_e(t)}{m_e}+\frac{p_h(t)}{m_h}\right\}U_{ex}|\Psi\rangle \tag{48}$$

We have for $P=0$:

$$U_{ex}^{-1}pU_{ex}=p+[iS,p]=p+i\left[\sum_{K,q}C_{K+q}^{+}C_K\left(f_{ex}^{*}b_{-q}^{+}+f_{ex}b_q\right),P-\sum_q\hbar\omega q b_q^{+}b_q\right]$$
$$=p-i\hbar\omega\sum_{K,q}qC_{K+q}^{+}C_K\left(f_{ex}b_q-f_{ex}^{*}b_{-q}^{+}\right) \tag{49}$$

Therefore:

$$R(\hbar\Omega)=\left(\frac{e}{\hbar\Omega}\right)^2\int_{-\infty}^{0}dt\ e^{-it(i\varepsilon+\hbar\Omega)}\langle\Psi|\ E.\left\{\frac{p_e}{m_e}+\frac{p_h}{m_h}-\frac{i\hbar\omega}{\mu}\sum_{K,q_{//}}q_{//}C_{K+q_{//}}^{+}C_K\left(f_{ex}b_{q_{//}}-f_{ex}^{*}b_{-q_{//}}^{+}\right)\right\}\times$$
$$E.\left\{\frac{p_e(t)}{m_e}+\frac{p_h(t)}{m_h}-\frac{i\hbar\omega}{\mu}\sum_{K,q_{//}}q_{//}C_{K+q_{//}}^{+}(t)C_K(t)\left(f_{ex}b_{q_{//}}(t)-f_{ex}^{*}b_{-q_{//}}^{+}(t)\right)\right\}|\Psi\rangle \tag{50}$$

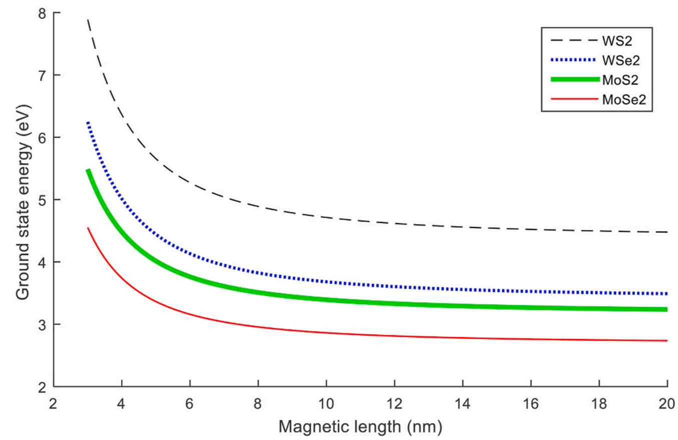

Fig. 2. Exciton-polaron ground state energy versus the length scale l_B of magnetic barrier for various 1Ls TMDs.

By using the relation $\frac{dC(t)}{dt}=i\,[H,C(t)]$, the time dependence of the different operators is

Obtained as:

$$C_{K+q}^{+}(t)C_K(t)=C_{K+q}^{+}C_K\ e^{-it\left(\lambda_K-\lambda_{K+q}\right)}\ :\ b_{-q}^{+}(t)=b_{-q}^{+}\ e^{it\hbar\omega}\ and\ p\ (t)=p\ (0)=p \tag{51}$$

with the previous relation and after averaging with respect to Eq. (29), the real part is written as:

$$\mathrm{Re}R(\hbar\Omega)=\left(\frac{e}{\hbar\Omega}\right)^2\int_{-\infty}^{0}dt\ e^{-it(i\varepsilon+\hbar\Omega)}\left\{\frac{2\hbar^2E^2K^{*2}}{M^2}-\frac{\hbar^2E^2\left(m_e^2+m_h^2\right)}{m_e^2m_h^2a^2}+\frac{\hbar^2\omega^2}{\mu^2}\sum_{q_{//}}\left(E.\ q_{//}\right)^2f_{ex}f_{ex}^{*}\ e^{-itg}\right\} \tag{52}$$

where

$$g=\left(\lambda_K-\lambda_{K+q_{//}}-\hbar\omega\right) \tag{53}$$

We consider the ratio of frequencies $\chi=\Omega/\omega$. The optical absorption coefficient reads:

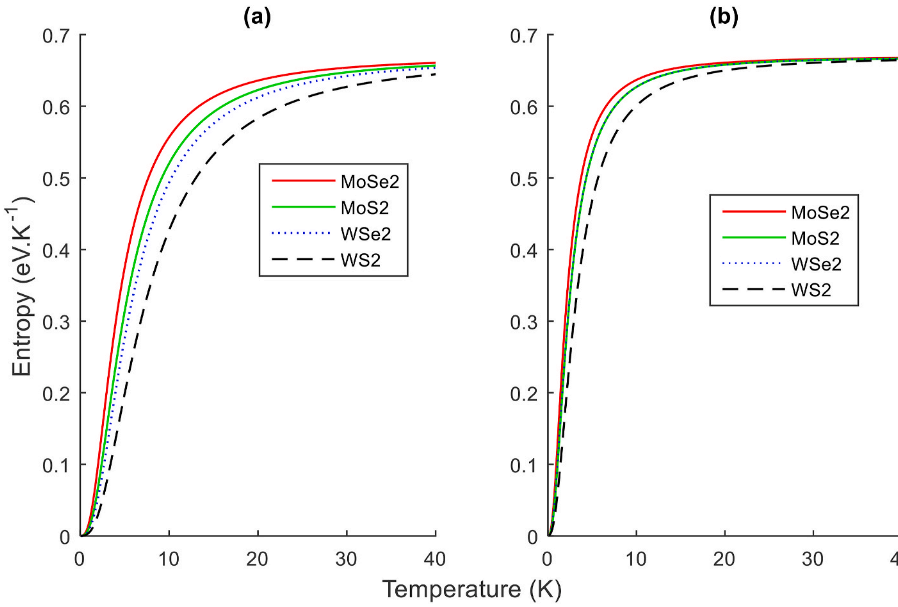

Fig. 3. Exciton-polaron entropy as function of the temperature for various 1L TMDs at $j = 1.1$ (a) $l_B = 5\ nm$ and (b) $l_B = 50\ nm$.

$$\begin{aligned}\Gamma(\chi) &= \frac{\pi e^2}{cn\varepsilon_0\hbar(\hbar\omega)^2\chi}\left\{\frac{2\hbar^2K^{*2}}{M^2}-\frac{\hbar^2\left(m_e^2+m_h^2\right)}{m_e^2m_h^2a^2}\right\}\delta(\chi)\\ &+\frac{\pi e^2\omega}{cn\varepsilon_0\mu^2E^2\chi}\sum_{q_{//}}\left(E.\,q_{//}\right)^2 f_{ex}f_{ex}^*\,\delta\left[-\frac{\hbar^2}{2M}\left(q_{//}^2+2kq_{//}\cos\theta\right)+\hbar\omega(\chi-1)\right]\end{aligned} \tag{54}$$

Transforming the summation into an integration, one gets:

$$\begin{aligned}\Gamma(\chi) &= \frac{\pi e^2}{cn\varepsilon_0\hbar(\hbar\omega)^2\chi}\left\{\frac{2\hbar^2}{M^2}\left(k^2+\frac{1}{l_B^2}\right)-\frac{\hbar^2\left(m_e^2+m_h^2\right)}{m_e^2m_h^2a^2}\right\}\delta(\chi)\\ &+\frac{M\hbar\omega e^2\left(D_c^{op}-D_v^{op}\right)^2}{4\pi cn\varepsilon_0\eta u\hbar^2\mu^2\chi}\sin^2(\gamma)\int_0^{2\pi}d\theta\int_0^{\infty}dq_{//}\frac{q_{//}^4\ \delta\left[q_{//}^2+2kq_{//}\cos\theta-\frac{2M\hbar\omega(\chi-1)}{\hbar^2}\right]}{\frac{\hbar^4}{4M^2}\left(q_{//}^2+2kq_{//}\cos\theta\right)^2-(\hbar\omega)^2}\end{aligned} \tag{55}$$

γ is the angle between the field induced by incident photon (E) and the normal of TMD.

Let us take $q_0^2 = 2M\hbar\omega(\chi-1)/\hbar^2$ for $\chi > 1$;

We first integrate over $q_{//}$ in Eq. (55), it gives:

$$\begin{aligned}\Gamma(\chi) &= \frac{e^2\sqrt{\pi}}{cn\varepsilon_0\hbar(\hbar\omega)^2}\left\{\frac{2\hbar^2}{M^2}\left(k^2+\frac{1}{l_B^2}\right)-\frac{\hbar^2\left(m_e^2+m_h^2\right)}{m_e^2m_h^2a^2}\right\}\frac{\exp(-\chi^2/\alpha^2)}{|\alpha|\chi}+\frac{M\hbar\omega e^2\left(D_c^{op}-D_v^{op}\right)^2}{8\pi cn\varepsilon_0\eta u\hbar\mu^2}\times\\ &\frac{\sin^2(\gamma)}{\chi}\int_0^{2\pi}\frac{d\theta}{\sqrt{\hbar^2k^2\cos^2\theta+2M\hbar\omega(\chi-1)}}\left\{\frac{q_3^4}{\frac{\hbar^4}{4M^2}\left(q_3^2+2kq_3\cos\theta\right)^2-(\hbar\omega)^2}+\frac{q_4^4}{\frac{\hbar^4}{4M^2}\left(q_4^2+2kq_4\cos\theta\right)^2-(\hbar\omega)^2}\right\}\end{aligned} \tag{56}$$

where

$$q_3 = -k\cos\theta+\frac{1}{\hbar}\sqrt{\hbar^2k^2\cos^2\theta+2M\hbar\omega(\chi-1)}\ :\ q_4 = -k\cos\theta-\frac{1}{\hbar}\sqrt{\hbar^2k^2\cos^2\theta+2M\hbar\omega(\chi-1)} \tag{57}$$

This leads to:

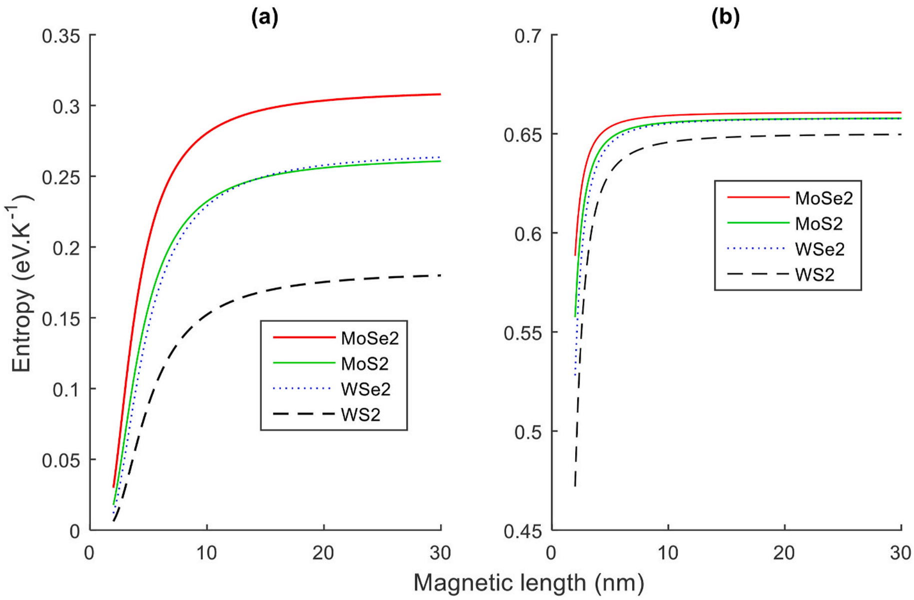

Fig. 4. Excitonic polaron entropy versus the length scale (l_B) of the magnetic barrier for various monolayers TMDs for $j = 1.1$ (a) $T = 2K$ and (b) $T = 20K$.

$$\Gamma(\chi) = \frac{e^2\sqrt{\pi}}{cn\varepsilon_0\hbar(\hbar\omega)^2}\left\{\frac{2\hbar^2}{M^2}\left(k^2+\frac{1}{l_B^2}\right) - \frac{\hbar^2\left(m_e^2+m_h^2\right)}{m_e^2m_h^2a^2}\right\}\frac{\exp(-\chi^2/\alpha^2)}{|\alpha|\chi} + \frac{Me^2\left(D_c^{op}-D_v^{op}\right)^2}{8\pi cn\varepsilon_0\eta u\hbar(\hbar\omega)\mu^2}\times \frac{\sin^2(\gamma)}{\chi^2(\chi-2)}\int_0^{2\pi}d\theta\,\frac{16k^4\cos^4\theta + 32M\hbar\omega(\chi-1)k^2\cos^2\theta/\hbar^2 + 4M^2(\hbar\omega)^2(\chi-1)^2/\hbar^4}{\sqrt{\hbar^2k^2\cos^2\theta + 2M\hbar\omega(\chi-1)}} \tag{58}$$

The final expression of the absorption coefficient is obtained by integrating the previous equation over θ. It is proportional to the photon's incidence, the photon's frequency, the magnetic length and the TMD's parameters.

3. Results and discussion

We have derived the analytical expression of Tsallis entropy, mobility, lifetime and optical absorption coefficient of an exciton-polaron in 1L TMDs submitted to a magnetic barrier. The Fröhlich unit and the data of each material are given in Table 1.

Fig. 2 displays the fundamental state energy of an exciton-polaron versus magnetic length for different monolayers. As we can see from this figure, the exciton polaron ground state energy is very sensitive to the applied magnetic field in all considered 2D materials. The variation of magnetic field in the increasing direction enhances the ground state energy of the system. Therefore, since the magnetic length is a function of $1/B$, the exciton-polaron interaction becomes stronger as well as the magnetic length reduces and inversely. It is seen that the fundamental state energy drops with the expansion of l_B and there is a shift between the monolayers. The magnetic field plays an interesting role on the energy of an exciton-polaron in TMDs. Due to magnetic barrier, the interaction between particles is strengthened and the exciton-polaron is more confined in TMDs. This result is in accordance with what was found by Myoung et al. [52]. The authors have proved that magnetic gate is suitable for use as base elements for one-electron tunneling systems or spin-polarized devices. In fact, the decrease in the length scale enhances the barrier height and the exciton-polaron is well confined in the ground state. This assumption is found spectacularly in systems like TMDs where the electronic structure changes abruptly when they are stripped down from few to a single atomic layer [65]. WS_2 has the highest ground state energy and $MoSe_2$ the lowest one.

In Fig. 3, we have plotted the entropy of an excitonic polaron versus temperature for some monolayers respectively for $l_B = 5\ nm$ Fig. 3a and $l_B = 50\ nm$ Fig. 3b. Each figure shows the increase of entropy with temperature and an approximately change in evolution for all considered monolayers when the magnetic length is modified. From the figures, it becomes evident that the entropy for all compounds expands up to T = 25 K and then remains constant. The entropy starts from zero and increases until reaches the thermodynamic equilibrium which confirms the principle of the third law of thermodynamic and it is in accordance with physics laws and the work of [19]. The main explanation of the increasing entropy can also be due to the fact that phonons cause random fluctuations of energy from each local state. These fluctuations break the coherence of the excitonic states and lead to a process of relaxation at the origin of various phenomena like decoherence. Then, as a result, the system is decoherent for T < 25 K, coherent for T > 25 K and $MoSe_2$ has the highest entropy. From Fig. 3b, it can be seen that the magnetic barrier modifies the entropy behavior. We may see that, the entropy of the system is very sensitive to monolayers TMDs, magnetic length and temperature. We find that the magnetic barrier controls the system disorder. This result is in accordance with the one obtained by Fobasso et al. [66].

We observe in Fig. 4 that entropy increases and reaches an equilibrium state with the enhancement of magnetic length. The higher the magnetic length, the longer the disorder until a certain period and then, coherence can be restored in the system. Then it is possible to control the information of the system. This means that it is possible to encode quantum information on the high-frequency vibrations of excitonic

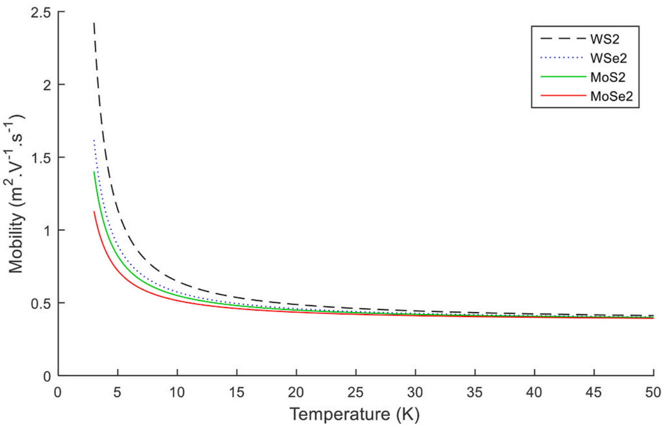

Fig. 5. Exciton-polaron mobility versus the temperature for different 1L TMD materials at $l_B = 5\,nm$.

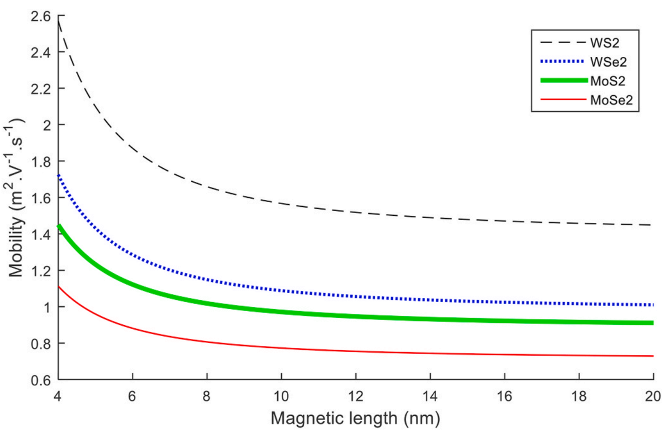

Fig. 6. Exciton-polaron mobility versus the magnetic barrier length (l_B) for different 1L TMD materials at T = 5 K.

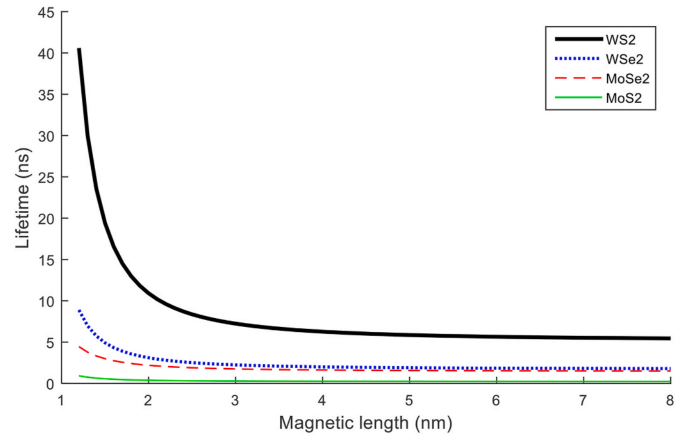

Fig. 7. Exciton-polaron lifetime versus the length scale (l_B) of the magnetic barrier for different monolayers TMDs.

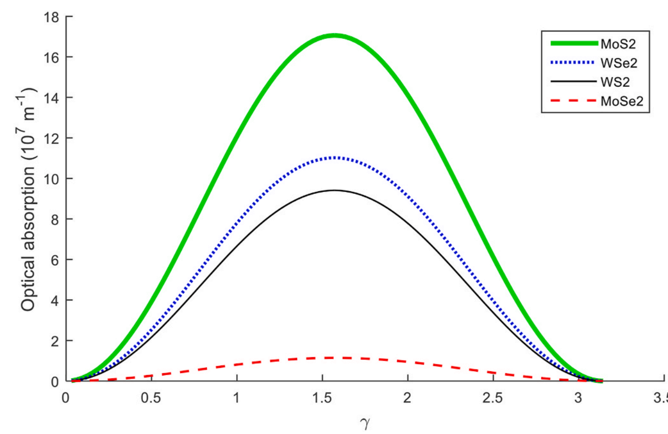

Fig. 8. Optical absorption coefficient versus the incidence angle of photon for different TMDs at $\chi = 2.01$ and $l_B = 10\,nm$.

polaron in quantum communication protocol. The exciton-polaron is confined in TMD materials when l_B decreases (as seen in Fig. 2) and the disorder can be control by the temperature and magnetic length. It is well recognized that an accumulation of entropy signifies the deficiency of information within the system. The variation of the magnetic length plays an essential role in the coherence control of systems [67–69].

In Fig. 5, we present the exciton-polaron mobility as function of the temperature. It is observed that the mobility of exciton-polaron decreases with the increase in temperature. This behavior is understood when we look at the entropy. In fact, as the temperature enhances that generates disorder in excitonic network and then perturbs the motion of particles. In presence of temperature, the exciton-polaron has a random movement leading to the reduction of this transport property. Also, as for Fig. 3, at very high temperatures (T > 25 K) the mobility becomes constant and the movement of electron (hole) is dominated by high disorder contributing then to the lowest values of mobility. The result is in agreement with [70] and with Djomou et al. [71] who show that it is possible to accelerate the movement of a quasiparticle in nanostructures. Contrary to the entropy case, the highest mobility is obtained for WS_2 and the lowest for $MoSe_2$. In addition, Fig. 6 represents the mobility of an excitonic polaron versus magnetic length. It is observed that mobility decreases slowly with the magnetic length. As it was seen for energy, the exciton-polaron in TMDs is localized and its motion is modified by the magnetic barrier. In fact, from Eq. (15), it follows that low values of the magnetic length (high magnetic field) enhance the kinetic energy of exciton-polaron and as the magnetic length increases its influence on kinetic energy vanishes. One can say that for high values of the magnetic length, the magnetic barrier doesn't more act on the excitonic polaron mobility. Among the selected TMD materials, the mobility is most sensible for WS_2 and this result is in accordance with the one of Pouthier [72].

Fig. 7 presents the exciton-polaron lifetime as function of the magnetic length for the four TMDs. It is observed that the exciton-polaron lifetime decreases with the increase of the length scale. This is in agreement with [28]. This can be explained through the confinement of exciton motion. In the presence of magnetic field, the distance between particles is reduced, the binding energy is enhanced and electron (hole) better interacts with the structure. This interaction is reduced when enhances the magnetic length and then the existence of excitonic polaron becomes weak in the barrier. We can confirm that the change in exciton-polaron can alter the interplay effects with phonons, thus affects the decay time. The more the particle is confined in the barrier, the higher the mobility and the higher the lifetime. As it was predicted with mobility, the monolayer with long decay time is WS_2. At low magnetic length, the exciton-polaron has a long decay time and great energy, this result is in agreement with [47,48]. These characteristics make the TMD sheets a robust system for performing indirect exciton-polaron condensation in space.

Fig. 8 displays the behavior of the optical absorption as function of the photon incidence. It is observed that the peak of absorption appears at $\gamma = \pi/2$ corresponding to the incident photon in the plane. In fact, for this value of the angle, the total strength of the field induced by incident photon interactes with exciton-polaron in TMD materials. Also, the lowest absorption of photon by excitonic polaron is obtained for

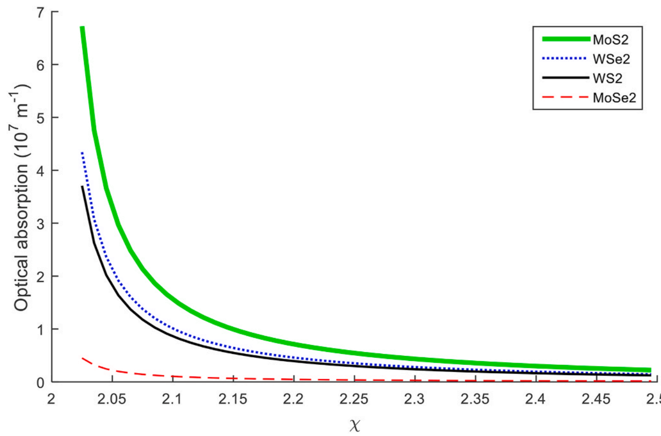

Fig. 9. Optical absorption coefficient as function of the incident photon energy for different TMDs at $l_B = 10\,nm$ and $\gamma = \pi/2$.

incidence normal to the plane. The result indicates that as the angle varies from the normal to $\pi/2$, the stronger the interaction with photon and then increases the probability of absorbing photon. Moreover, from Eq. (58) one can see that for $\chi < 2$ it is negative values of absorption coefficient and also $\chi = 2$ leads to $\Gamma \rightarrow \infty$. It is also convenient to take $\chi > 1 - (\hbar^2 k^2 \cos^2\theta / 2M\hbar\omega)$ due to the presence of the square root. Therefore, the result reveals that the absorption of light by exciton-polaron starts when the photon energy is more than twice phonon energy ($\chi > 2$) and it falls as shown Fig. 9. This is in agreement with the recent work of [62]. We can say that exciton-polaron may have similar properties as polaron alone. The result also quantifies the photonic impact on the exciton. This result is linked with the experimental one of Lengers et al. [73]. The optical absorption coefficient is highest for MoS_2 and lowest for $MoSe_2$.

Fig. 10 presents the reduction of the optical absorption with the increase of magnetic length since it is proportional to $1/(l_B^2)$ as shows Eq. (58). The spectra of absorption in 1Ls TMDs exhibits strong signatures of the unusually pronounced exciton-polaron interference in such materials of short magnetic length. This good absorption at low magnetic length delivers a useful utility for quantifying absorption spectra in popular monolayers materials. This result is in agreement with existing theoretical explanations of optical devices that are focused mainly on basic excitonic resonances by using a simple Wannier scheme for correlated electron-hole couples [74–76] or the Ab-initio Bethe-Salpeter equation [77–79]. But in these works, the linear form of the excitonic resonance tends to be incorporated phenomenologically like a Lorentzian. As the source of line forms is diverse [80], some works are dedicated to the description of the impact of excitonic phonon interaction [81]. Here, we add the influence of magnetic barrier on the spectra since the presence of magnetic field enhances the probability of absorbing the photon by exciton-polaron in the ground state. Thus, the results show that as the electron and hole need more phonon energy to absorb light, the absorption can be adjusted by the magnetic barrier.

4. Conclusion

The exciton-polaron properties have been studied in monolayers TMDs. We precisely investigated the Tsallis entropy, the mobility, the entropy and the optical absorption coefficient of the system through magnetic barrier. The results are obtained for different TMD materials ($MoSe_2$, WSe_2, WS_2, MoS_2) for comparison. We found that the exciton-polaron is confined in the magnetic barrier and the energy of exciton-polaron is lower than that of the polaron states. This favorable energy could have impact on other properties of the excitonic polaron. Also, the entropy increases with temperature and approximately changes in evolution for the different monolayers when the magnetic length is modified. We showed that the entropy of the system is very sensitive to monolayers TMDs, magnetic length and temperature. The magnetic barrier can be used to restore order in a system subject of thermal perturbation, control experimental disorder and influence quantitative measurements. It is seen that the exciton-polaron lifetime decreases with the increase of the length scale. We confirm that the transport of exciton-polaron affects the decay time. A good absorption at short magnetic length supplies a valuable tool for quantifying the absorption spectra in widely used single-layer substrates. The orientation of the field induced by the incident photon modifies the amplitude of the optical absorption coefficient. These results are useful for the improvement of electronic and optic devices.

Declaration of competing interest

The authors declare that they have no known competing financial interests or personal relationships that could have appeared to influence the work reported in this paper.

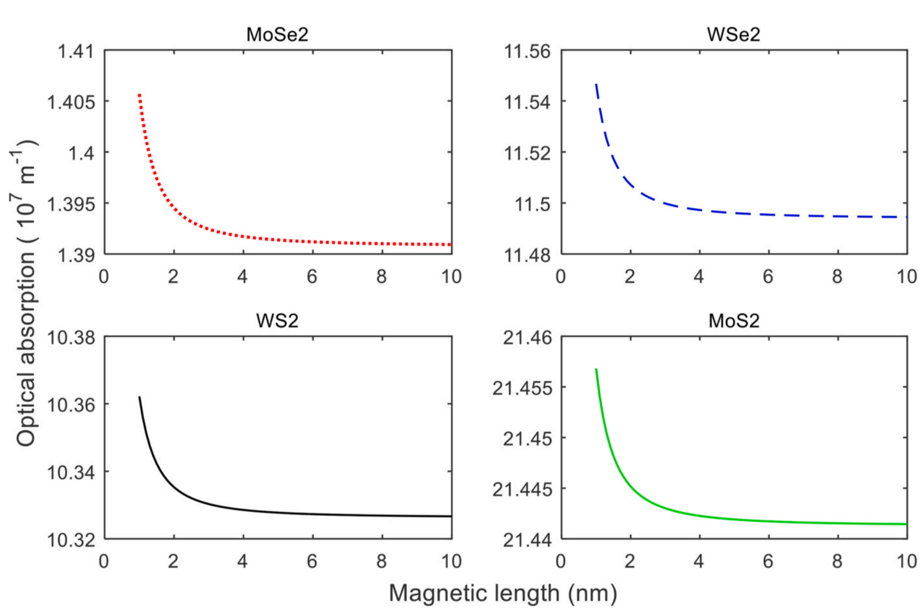

Fig. 10. Optical absorption coefficient versus the magnetic length for various TMDs at $\chi = 2.01$ and $\gamma = \pi/2$.

Acknowledgments

LMP acknowledges ANID through Convocatoria Nacional Subvención a Instalación en la Academia Convocatoria Año 2021, Grant SA77210040. DL acknowledges partial financial support from Centers of Excellence with BASAL/ANID financing, Grant AFB180001, CEDENNA. CKS acknowledges support from the Deutscher Akademischer Austauchdienst German Academic Exchange Service through the Staff Exchange Fellowships in Sub-Saharan-Africa.

References

[1] S. Ayari, A. Smiri, A. Hichri, S. Jaziri, T. Amand, Radiative lifetime of localized excitons in transition-metal dichalcogenides, Phys. Rev. B 98 (2018), 205430.
[2] J.V. Nguepnang, C. Kenfack-Sadem, A. Kenfack-Jiotsa, C. Guimapi, A.J. Fotue, A. E. Merad, Electron-phonon coupling contribution on the optical absorption and the dynamic of exciton-polaron in monolayer transition meta dichalcogenides, Opt. Quant. Electron. 53 (2021) 654.
[3] S.V. Mandyam, H.M. Kim, M. Drndic, Large area few-layer TMD film growths and applications, J. Phys. Mater. 3 (2020), 024008.
[4] H.G. Ji, P.S. Fernandez, U. Erkilic, H. Ago, Stacking orientation-dependent photoluminescence pathways in artificially stacked bilayer WS_2 nanosheets grown by chemical vapor deposition: implications for spintronics and valleytronics, ACS Appl. Nano Mater. 4 (2021) 3717–3724.
[5] A.J. Pearce, G. Burkard, Electron spin relaxation in a transition metal dichalcogenide quantum dot, 2D Mater. 4 (2017), 025114.
[6] N.D. Hien, C.V. Nguyen, N.N. Hieu, S.S. Kubakaddi, C.A. Duque, M.E. Mora-Ramos, L. Dinh, T.N. Bich, H.V. Phuc, Magneto-optical transport properties of monolayer transition metal dichalcogenides, Phys. Rev. B 101 (2020), 045424.
[7] Z. Wang, J. Shan, K.F. Mak, Valley and spin polarized Landau levels in monolayer WSe_2, Nat. Nanotechnol. 12 (2017) 144–149.
[8] C.V. Nguyen, N.N. Hieu, D. Muoi, C.A. Duque, E. Feddi, H.V. Nguyen, L.T. T. Phuong, B.D. Hoi, H.V. Phuc, Linear and nonlinear magneto-optical properties of monolayer MoS_2, J. Appl. Phys. 123 (2018), 034301.
[9] W. Liu, Z. Lin, S. Tian, Y. Huang, H. Xue, K. Zhu, C. Gu, Y. Yang, J. Li, Plasmonic effect on the magneto-optical property of monolayer WS_2 studied by polarized-Raman spectroscopy, Appl. Sci. 11 (2021) 1599.
[10] J. Forste, N.V. Tepliakov, S.Y. Kruchinin, J. Lindlau, V. Funk, M. Forg, K. Watanable, T. Taniguchi, A.S. Baimuratov, A. Hogele, Exciton g-factors in monolayer and bilayer WSe_2 from experiment and theory, Nat. Commun. 11 (2020) 1–8.
[11] E. Liu, J.V. Baren, C.T. Liang, T. Taniguchi, K. Watanabe, N.M. Gabor, Y.C. Chang, C.H. Lui, Multipath optical recombination of intervalley dark excitons and trions in monolayer WSe_2, Phys. Rev. Lett. 124 (2020), 196802.
[12] Z.W. Wang, W.P. Li, Y. Xia, R.Z. Li, Z.Q. Li, Influence of exciton-phonons coupling on the exciton binding energy in monolayer transition metal dichalcogenides, Appl. Phys. Lett. 110 (2017), 231603.
[13] E. Jung, J.C. Park, Y.S. Seo, J.H. Kim, J. Hwang, Y.H. Lee, Unusually large exciton binding energy in multilayered 2H-MoTe2, Sci. Rep. 12 (2022) 1–10.
[14] A.J. Chaves, R.M. Ribeiro, T. Frederico, N.M.R. Peres, Excitonic effects in the optical properties of 2D materials: an equation of motion approach, 2D Mater. 4 (2017), 025086.
[15] A.V. Stier, N.P. Wilson, K.A. Velizhanin, J. Kono, X. Xu, S. Crooker, Magneto-optics of exciton Rydberg states in a monolayer semiconductor, Phys. Rev. Lett. 120 (2018), 057405.
[16] J. Zipfel, J. Holler, A.A. Mitioglu, M.V. Ballottin, P. Nagler, A.V. Stier, T. Taniguchi, K. Watanabe, S.A. Crooker, P.C.M. Christiansen, T. Korn, A. Chernikov, Spatial extent of the excited exciton states in WS_2 monolayers from diamagnetic shifts, Phys. Rev. B 98 (2018), 075438.
[17] S. Helmrich, R. Schneider, A.W. Achtstein, A. Arora, B. Herzog, S.M. de Vasconcellos, M. Kolarczik, O. Schops, R. Bratschitsch, U. Woggon, N. Owschimikow, Exciton-phonon coupling in mono-and bilayer $MoTe_2$, 2D Mater. 5 (2018), 045007.
[18] D. Christiansen, M. Selig, G. Berghauser, R. Schmidt, I. Niehues, R. Schneider, A. Arora, S.M. de Vasconcellos, R. Bratschitsch, E. Malic, A. Knorr, Phonon sidebands in monolayer transition metal dichalcogenides, Phys. Rev. Lett. 119 (2017), 187402.
[19] I. Niehues, R. Schmidt, M. Druppel, P. Marauhn, D. Christiansen, M. Selig, G. Berghauser, D. Wigger, R. Schneider, L. Braasch, R. Koch, A. Castellanos-Gomez, T. Kuhn, A. Knorr, E. Malic, M. Rohlfing, S.M. de Vasconcellos, R. Bratschitsch, Strain control of exciton phonon coupling in atomically thin semiconductors, Nano Lett. 18 (2018) 1751–1757.
[20] W.P.D. Wong, J. Yin, B. Chaudhary, X.Y. Chun, D. Cortecchia, S.-Z.A. Lo, A. C. Grimsdale, O.F. Mohammed, G. Lanzani, C. Soci, Large polaron self-trapped states on three dimensional metal Halide Perovskites, ACS Materials Lett 2 (2020) 20–27.
[21] A. Simbula, R. Pau, Q. Wang, F. Liu, V. Sarritzu, S. Lai, M. Lodde, F. Mattana, G. Mulla, A.G. Lehmann, I.D. Spanopoulos, M.G. Kanatzidis, D. Marongiu, F. Quochi, M. Saba, A. Mura, G. Bongiovanni, Polaron plasma in equilibrium with bright excitons in 2D and 3D hybrid Perovskites, Adv. Opt. Mater. 9 (2021), 2100295.
[22] D. Li, C. Trovatello, S.D. Conte, M. Nub, G. Soavi, G. Wang, A.C. Ferrari, G. Cerullo, T. Brixner, Exiton phonon coupling strength in single layer $MoSe_2$ at room temperature, Nat. Commun. 12 (2021) 954.
[23] T. Wang, M.S. Niu, J.J. Guo, K.N. Zhang, Z.C. Wen, J.Q. Liu, C.C. Qin, X.T. Hao, 3D charge transport pathway in organic solar cells via incorporation of discotic liquid crystal columns, Solar RRL 4 (2020), 2000047.
[24] S. Shree, M. Semina, C. Robert, B. Han, T. Amand, A. Balocchi, M. Manca, E. Courtade, X. Marie, T. Taniguchi, K. Watanabe, M.M. Glazov, B. Urbaszek, Observation of exciton phonon coupling in $MoSe_2$ monolayers, Phys. Rev. B 98 (2018), 035302.
[25] C. Trovatello, H.P.C. Miranda, A.M. Sanchez, R.B. Varillas, C. Manzoni, L. Moretti, L. Ganzer, M. Maiuri, J. Wang, D. Dumcenco, A. Kis, L. Wirtz, A. Marini, G. Soavi, A.C. Ferrari, G. Cerullo, D. Sangalli, S.D. Conte, Strongly coupled coherent phonons in single-layer MoS_2, ACS Nano 14 (2020) 5700–5710.
[26] S. Ono, T. Ogura, Anomalous energy shift of laterally confined two dimensional excitons, J. Appl. Phys. 124 (2018), 034301.
[27] Y. Liu, H. Li, C. Qiu, X. Hu, D. Liu, Layer dependent signatures for exciton dynamics in monolayer and multilayer WSe_2 revealed by fluorescence lifetime imaging measurement, Nano Res. 13 (2020) 661–666.
[28] Y.J. Zheng, Y. Chen, Y.L. Huang, P.K. Gogoi, M.Y. Li, L.J. Li, P.E. Trevisanutto, Q. Wang, S.J. Pennycook, A.T.S. Wee, S.Y. Quek, Point defects and localized excitons in 2D WSe_2, ACS Nano 13 (2019) 5.
[29] L. Du, M. Liao, J. Tang, Q. Zhang, H. Yu, R. Yang, K. Watanable, T. Taniguchi, D. Shi, Q. Zhang, G. Zhang, Strongly enhanced exciton phonon coupling in two dimensional WSe_2, Phys. Rev. B 97 (2018), 235145.
[30] M.C. Gelvez-Rueda, E.M. Hutter, D.H. Cao, N. Renaud, C.C. Stoumpos, J.T. Hupp, T.J. Savenije, M.G. Kanatzidis, F.C. Grozema, Interconversion between free charges and bound excitons in 2D hybrid lead Halide Perovskites, J. Phys. Chem. C 121 (2017) 47.
[31] M. Tiotsop, A.J. Fotue, G.K. Fautso, C.S. Kenfack, H.B. Fotsin, L.C. Fai, Decoherence time, hydrogenic-like impurity effect and Shannon entropy on polaron in RbCl triangular quantum dot qubit, Superlattice. Microst. 103 (2017) 70–77.
[32] S.C. Kenfack, A.J. Fotue, M.F.C. Fobasso, G.N. Bawe, L.C. Fai, Shannon entropy and decoherence of polaron in asymmetric polar semiconductor quantum wire, Superlattice. Microst. 111 (2017) 32–44.
[33] D.V. Tuan, M. Yang, H. Dery, Coulomb interaction in monolayer transition metal dichalcogenides, Phys. Rev. B 98 (2018), 125308.
[34] R. Khordad, S. Goudarzi, H. Bahramiyan, Effect of temperature on lifetime and energy states of bound polaron in asymmetrical Gaussian quantum well, Indian J. Phys. 90 (2016) 659–664.
[35] Z. Li, The ground state lifetime of polaron in a two-dimensional quantum pseudodot system, Indian J. Phys. 93 (2018) 707–711.
[36] T. Mueller, E. Mallic, Exciton physics and device application of two-dimensional transition metal duchalcogenide semiconductors, npj 2D Mater, Apple 2 (2018) 1–12.
[37] X. Xi, Z. Wang, W. Zhao, J.H. Park, K.T. Law, H. Berger, L. Forro, J. Shan, K.F. Mak, Ising pairing in superconducting $NbSe_2$ atomic layers, Nat. Phys. 12 (2016) 139–143.
[38] Z. Fei, T. Palomaki, W. Wu, S. Zhao, X. Cai, B. Sun, P. Nguyen, J. Finney, X. Xu, D. H. Cobden, Edge conduction in monolayer WTe_2, Nat. Phys. 13 (2017) 677–682.
[39] Z.E. Eroglu, O. Comegys, L.S. Quintanar, N. Azam, S. Elafandi, M.M. Samani, A. Boulesbaa, Ultrafast dynamics of exciton formation and decay in two-dimensional tungsten disulfide 2D-WS_2 monolayers, Phys. Chem. Chem. Phys. 22 (2020) 17385–17393.
[40] A. Rodek, T. Hahn, J. Kasprzak, T. Kazimierczuk, K. Nogajewski, K.E. Polczynska, K. Watanabe, T. Taniguchi, T. Kuhn, P. Machnikowski, M. Potemski, D. Wigger, P. Kossacki, Local field effects in ultrafast light-matter interaction measured by pump-probe spectroscopy of monolayer $MoSe_2$, Nanophotonics 10 (2021) 2717–2728.
[41] Y. Hu, F. Zhang, M. Titze, B. Deng, H. Li, G.J. Cheng, Straining effects in MoS_2 monolayer on nanostructured substrates: temperature dependent photoluminescence and exciton dynamics, Nanoscale 10 (2018) 5717–5724.
[42] Y.Y. Yue, H.Y. Wang, L. Wang, L.Y. Zhao, H. Wang, B.R. Gao, H.B. Sun, Direct observation of room temperature intravalley coherent coupling processes on monolayer MoS_2, Laser Photon. Rev. 16 (2022), 2100343.
[43] H. Liu, A. Pau, D.K. Efimkin, Hybrid dark excitons in monolayer MoS_2, Phys. Rev. B 104 (2021), 165411.
[44] H. Shi, R. Yan, S. Bertolazzi, J. Brivio, B. Gao, A. Kis, D. Jena, H.G. Xing, L. Huang, Exciton dynamics in suspended monolayer and few layer MoS_2 2D crystals, ACS Nano 7 (2013) 1072–1080.
[45] F. Wu, T. Lovorn, A.H. MacDonald, Theory of optical absorption by interlayer excitons in transition metal dichalcogenides heterobilayers, Phys. Rev. B 97 (2018), 035306.
[46] P. Rivera, J.R. Schaibley, A.M. Jones, J.S. Ross, S. Wu, G, P. Klement, K. Seyler, G. Clark, N.J. Ghimire, J. Yan, D.G. Mandrus, W. Yao, X. Xu, Observation of long-lived interlayer excitons in monolayer $MoSe_2$ –WSe_2 heterostructures, Nat. Commun. 6 (2015) 6242.
[47] Q.H. Wang, K. Zadeh, K. Kourosh, C. Andras, N.J. Strano, S. Michael, Electronics and optoelectronics of two-dimensional transition metal dichalcogenides, Nat. Nanotechnol. 7 (2012) 699–712.
[48] P.F. Li, Z.W. Wang, Optical absorption of Frohlich polaron in monolayer transition metal dichalcogenides, J. Appl. Phys. 123 (2018), 204308.
[49] A. Thilagam, Excitonic polarons in low dimensional transition metal dichalcogenides, Phys. B Condens. Matter 464 (2015) 44–50.

[50] S. Zielinska-Raczynska, D.A. Fishman, C. Faugeras, M.M.P. Potemski, P.H.M. V. Loosdrecht, K. Karpinski, G. Czajkowski, D. Ziemkiewicz, Magneto-excitons in Cu_2O: theoretical model from weak to high magnetic fields, New J. Phys. 21 (2019), 103012.

[51] G. Kankan Cong, N. Timothy, J. Kono, Excitons in magnetic fields, Encyclo. Modern Opt. II 2 (2018).

[52] N. Myoung, G. Ihm, S. Lee, Transport in armchair graphene nanoribbons modulated by magnetic barriers, Physica 42 (2010) 2808–2811.

[53] S. Ghosh, M. Sharma, Electron optics with magnetic vector potential barriers in graphene, J. Phys. Condens. Matter 21 (2009), 292204.

[54] V.K. Kozin, V.A. Shabashow, A.V. Kavokin, I.A. Shelykh, Anomalous exciton Hall effect, Phys. Rev. Lett. 126 (2021), 036801.

[55] C. Kenfack-Sadem, S. Mounbou, S.I. Fewo, M.F.C. Fobasso, A.J. Fotue, L.C. Fai, Optical absorption and Tsallis entropy of polaron in monolayer graphene, J. Low Temp. Phys. 200 (2020) 173–186.

[56] R. Khordad, H.R.R. Sedehi, Study of non-extensive entropy of bound polaron in monolayer graphene, Indian J. Phys. 92 (2018) 979–984.

[57] R. Khordad, Ar Firoozi, H.R.R. Sedehi, Simultaneous effects of temperature and pressure on the entropy and the specific heat of a three-dimensional quantum wire: Tsallis formalism, J. Low Temp. Phys. 202 (2021) 185–195.

[58] R. Khordad, H.R.R. Sedehi, Magnetic susceptibility of graphene in non-commutative phase-space: extensive and non-extensive entropy, Eur. Phys. J. A 134 (2019) 133.

[59] D. Kozawa, R. Kumar, A. Carvalho, K.K. Amara, W. Zhao, S. Wang, M. Toh, R. M. Ribeiro, A.H. Castro Neto, K. Matsuda, G. Eda, Photocarrier relaxation pathway in two dimensional semiconducting transition metal dichalcogenides, Nat. Commun. 5 (2014) 4543.

[60] M.F.C. Fobasso, C. Kenfack-Sadem, E. Baloitcha, A.J. Fotue, L.C. Fai, Lifetime and dynamics of polaron and bipolaron in graphene nanoribbon under laser, Eur. Phys. J. A 135 (2020) 471.

[61] J.T. Devreese, Frohlich Polarons: Lecture Course Including Detailed Theoretical Derivations, eighth ed., 2018. Antwerpen, Belgium.

[62] C. Kenfack-Sadem, A.K. Teguimfouet, A. Kenfack Jiotsa, R.M.K. Tsiaze, Dynamics and decoherence of exciton polaron in monolayer transition metal dichalcogenides, J. Electron. Mater. 50 (2021) 5.

[63] A.K. Teguimfouet, C.K. Sadem, J.V. Nguepnang, A.K. Jiotsa, K. Bhattacharyya, Relaxation and transport of excitonic polaron in monolayer transition metal dichalcogenides, Iran, J. Sci. Technol. Trans. Sci. 46 (2022) 717–730.

[64] Y. Xiao, Z.Q. Li, Z.W. Wang, Polaron effect on the bandgap modulation in monolayer transition metal dichalcogenides, J. Phys. Condens. Matter 29 (2017), 485001.

[65] A. Splendiani, L. Sun, Y. Zhang, T. Li, J. Kim, C.Y. Chim, G. Galli, F. Wang, Emerging photoluminescence in monolayer MoS_2, Nano Lett. 10 (2010) 1271–1275.

[66] M.F.C. Fobasso, A.J. Fotue, S.C. Kenfack, L.C. Fai, Thermal properties of magnetopolaron in GaAs delta potential under Rashba effect, Phys. E Low-dimens. Syst. Nanostruct. 118 (2020), 113941.

[67] A.V. Stier, N.P. Wilson, G. Clark, X. Xu, S.A. Crooker, Probing the influence of dielectric environment on excitons in monolayer WSe_2: insight from high magnetic fields, Nano Lett. 16 (2016) 7054–7060.

[68] A.A. Mitioglu, K. Galkowski, A. Surrente, L. Klopotowski, D. Dumcenco, A. Kis, D. K. Maude, P. Plochocka, Magnetoexcitons in large area CVD grown monolayer MoS_2 and $MoSe_2$ on sapphire, Phys. Rev. B 93 (2016), 165412.

[69] A.V. Stier, K.M. McCreary, B.T. Jonker, J. Kono, S.A. Crooker, Exciton diamagnetic shifts and valley Zeeman effects in monolayer WS_2 and MoS_2 to 65 tesla, Nat. Commun. 7 (2016), 10643.

[70] J. Moore Frost, Calculating polaron mobility in halide perovskites, Phys. Rev. B 96 (2017), 195202.

[71] J.R.D. Djomou, S.C. Kenfack, A.J. Fotue, M.F.C. Fobasso, L.C. Fai, Contribution of bulk and surface phonons to the properties of polaron in $Zn_{1-x}Cd_xSe/ZnSe$ heterojunction confined in a triangular potential, Physica B: Phys. Condens. Matter 548 (2018) 58.

[72] V. Pouthier, Quantum decoherence in finite size exciton phonon systems, J. Chem. Phys. 134 (2011), 114516.

[73] F. Lengers, T. Kuhn, D.E. Reiter, Theory of the absorption line shape in monolayer of transition metal dichalcogenides, Phys. Rev. B 101 (2020), 155304.

[74] G. Berghauser, E. Malic, Analytical approach to excitonic properties of MoS_2, Phys. Rev. B 89 (2014), 125309.

[75] E. Malic, M. Selig, M. Feierabend, S. Brem, D. Christiansen, F. Wendler, A. Knorr, G. Berghauser, Dark excitons in transition metal dichalcogenides, Phys. Rev. Mater. 2 (2018), 014002.

[76] L. Meckbach, T. Stroucken, S.W. Koch, Influence of the effective layer thickness on the ground state and excitonic properties of transition metal dichalcogenide systems, Phys. Rev. B 97 (2018), 035425.

[77] D.Y. Qiu, F.H. da Jornada, S.G. Louie, Screening and many body effects in two dimensional crystals: monolayer MoS_2, Phys. Rev. B 93 (2016), 235435.

[78] T. Deilmann, K.S. Thygesen, Dark excitations in monolayer transition metal dichalcogenides, Phys. Rev. B 96 (2017), 201113.

[79] M. Druppel, T. Deilmann, J. Noky, P. Marauhn, P. Kruger, M. Rohlfing, Electronic excitations in transition metal dichalcogenide monolayers from an LDA+GdW approach, Phys. Rev. B 98 (2018), 155433.

[80] G. Moody, C. Kavir Dass, K. Hao, C. Chen, L. Li, A. Singh, G. Tran, K. Clark, X. Xu, G. Berghauser, E. Malic, A. Knorr, X. Li, Intrinsic homogeneous linewidth and broadening mechanisms of excitons in monolayer transition metal dichalcogenides, Nat. Commun. 6 (2015) 8315.

[81] M. Selig, G. Berghauser, A. Raja, P. Nagler, C. Schuller, T.F. Heinz, T. Korn, A. Chernikov, E. Malic, A. Knorr, Excitonic linewidth and coherence lifetime in monolayer transition metal dichalcogenides, Nat. Commun. 7 (2016), 13279.